

## Observation of asymmetric fission in $^{204}\text{Pb}$ at low excitation energies

Vineet Kumar<sup>1,\*</sup>, K. Mahata<sup>1,2</sup>, Sangeeta Dhuri<sup>1,2</sup>, A. Shrivastava<sup>1,2</sup>, K. Ramachandran<sup>1</sup>, S. K. Pandit<sup>1</sup>, V. V. Parkar<sup>1,2</sup>, A. Kumar<sup>1</sup>, Arati Chavan<sup>3</sup>, P. C. Rout<sup>1,2</sup>, and Satbir Kaur<sup>1,2</sup>

<sup>1</sup>Nuclear Physics Division, Bhabha Atomic Research Centre, Mumbai - 400085, India

<sup>2</sup>Homi Bhabha National Institute, Anushaktinagar, Mumbai 400 094, India and

<sup>3</sup>Vivekanand Education Societys College of Arts, Science and Commerce, Mumbai 400071, India

### Introduction

The asymmetric fission of preactinides near the  $\beta$ -stability line was first observed in 1980s [1] but observation of dominant asymmetric fission of the neutron-deficient  $^{180}\text{Hg}$  isotope at ISOLDE [2] prompted a renewed theoretical and experimental interest in the fission of neutron-deficient nuclei in the preactinide region. The attempts to explain the new type of asymmetric fission include shell effects in prescission configurations associated with dinuclear structures or quadrupole deformed neutron shells in the fragments and fissioning nucleus [3]. A recent analysis [4] of the available experimental data on low energy asymmetric fission of neutron-deficient nuclei around Pb concludes a leading role played by the light-fragment proton configuration, which is in contrast to the dominance of neutron shells predicted earlier. In this work, we present the measurement of fission fragment (FF) mass distributions of  $^{204}\text{Pb}$  populated in the  $^7\text{Li}+^{197}\text{Au}$  reaction. The measured FF mass distributions is fitted with a quintuple gaussian function. The symmetric and asymmetric components are extracted from the data for all the excitation energies of compound nucleus.

### Experiment and data analysis details

A self supported target of  $^{197}\text{Au}$  having thickness  $\approx 280 \mu\text{g}/\text{cm}^2$  was bombarded with a  $^7\text{Li}$  beam of energy 30, 35 and 42 MeV at the BARC-TIFR Pelletron-LINAC facility. Two large area ( $12.5 \times 7.5 \text{ cm}^2$ ) multiwire proportional counters (MWPCs) were placed in a scattering chamber at distance of 24 cm at  $50^\circ$  and  $-121.5^\circ$  for the coincident detection of the fission fragments [5]. The time of flight data and position information were used to determine the fragment velocities. The emission angles, calculated from the position information, were used to obtain the linear momenta. Fragment masses were finally determined using the time-of-flight (TOF) difference method. Small corrections in the fragment mass due to their energy loss in the target were obtained on

an event-by-event basis in an iterative manner for all the possible fragments.

### Results and discussion

Figure 1 shows the FF mass distribution of  $^{204}\text{Pb}$  at  $E_{SP}^* = 22.3 \text{ MeV}$  (a),  $E_{SP}^* = 18.4 \text{ MeV}$  (b) and  $E_{SP}^* = 15.9 \text{ MeV}$  (c) where  $E_{SP}^*$  is the excitation energy above the saddle point. The measured FF mass distributions for  $^{204}\text{Pb}$  are fitted using 3 modes represented by Gaussian distributions. The Gaussian distributions for the light and heavy fragments for a given asymmetric mode are constrained to have same width and area, and their positions are constrained to add up to compound nucleus mass ( $A_{CN}$ ). The peak positions of the symmetric and asymmetric components as well as the width of symmetric component are left free for the fitting. The width of the asymmetric peaks was left free at the lowest energy and restricted to be more than its value at the lowest energy, at two higher energies. The symmetric and asymmetric components along with the total fit function used to extract the symmetric fraction are shown in Fig 1.

The symmetric peak position is observed at  $A_{CN}/2 = 102$  on all three energies as expected from the LDM. The asymmetric peak positions are observed at 79(125) and 95(109). These peaks corresponds to the proton number 32(50) and 38(44) assuming the unchanged Z/A ratio from CN to fission fragments. This observation highlight the influence of Z 36, 45 and 50 in asymmetric fission of preactinide nuclei.

Figure 2 shows the contribution of symmetric fission for  $^{204}\text{Pb}$  as a function of excitation energy at the saddle point ( $E_{SP}^*$ ). The contribution of symmetric fission fraction (symmetric/total) increases as a function of excitation energy at the saddle point. The contribution of asymmetric fission mode is around 60% at the lowest excitation energy. The extracted symmetric fission fraction is compared with the  $^{180,182,183,190}\text{Hg}$ ,  $^{178}\text{Pt}$ ,  $^{184,192,202}\text{Pb}$  and  $^{205,207,209}\text{Bi}$  measurements from Refs. [6–8]. The values of symmetric fission component shows different characteristic clustering for proton induced fission of  $^{205,207,209}\text{Bi}$  [8] and heavy ion induced fission of  $^{180,182,183,190}\text{Hg}$ ,  $^{178}\text{Pt}$ ,  $^{184,192,202}\text{Pb}$  [6, 7]. This could

\*Electronic address: vineetk@barc.gov.in

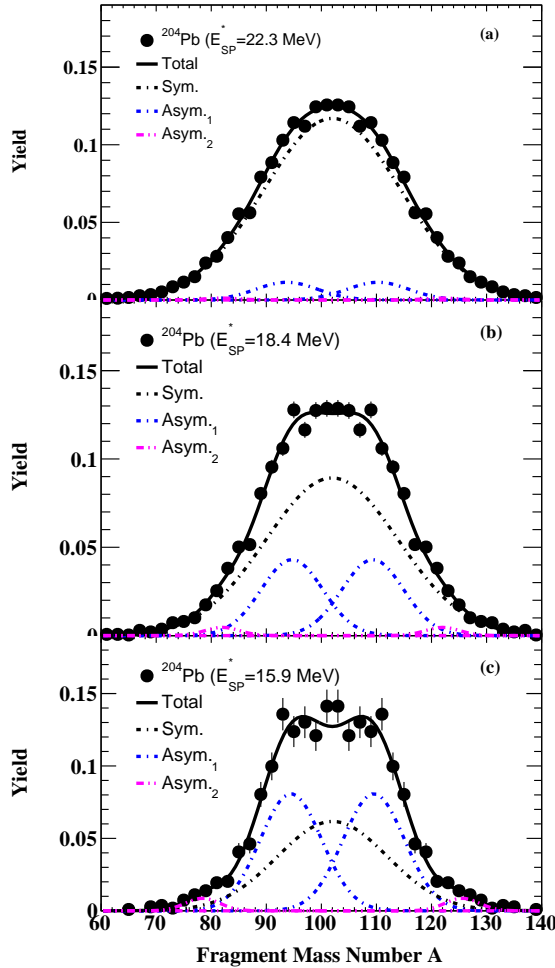


FIG. 1: Fission fragment mass distribution of  $^{204}\text{Pb}$  at  $E_{SP}^* = 22.3$  MeV (a),  $E_{SP}^* = 18.4$  MeV (b) and  $E_{SP}^* = 15.9$  MeV (c). The measured fission fragment mass distributions for  $^{204}\text{Pb}$  is fit with five gaussian function including one symmetric and two asymmetric modes.

be due to the entrance channel effect or larger shell corrections in the more neutron deficient nuclei.

The extracted symmetric fission fraction for  $^{204}\text{Pb}$  is also compared with the prediction from GEF model [9]. The GEF calculations under predict the symmetric fraction at the highest energy and predict different evolution of symmetric component as a function of  $E_{SP}^*$ . The  $^{204}\text{Pb}$  symmetric fraction matched well with the measured data for  $^{202}\text{Pb}$  [7] at overlapping energies. At lowest excitation energy the value of asymmetric fission is found to be  $\approx 60\%$  of total fission events.

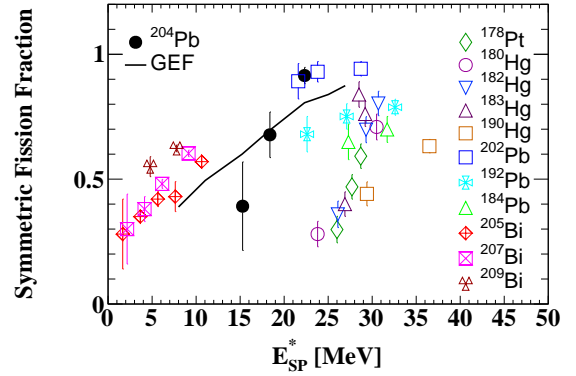


FIG. 2: The contribution of symmetric fission for  $^{204}\text{Pb}$  as a function of  $E_{SP}^*$  saddle point. The measured symmetric fission fraction is compared with the prediction of GEF model,  $^{178}\text{Pt}$  as well as  $^{180,182,183,190}\text{Hg}$  measurements from ref. [6],  $^{184,192,202}\text{Pb}$  measurements from ref. [7] and  $^{205,207,209}\text{Bi}$  measurements from ref. [8].

### Summary

The measured FF mass distribution of  $^{204}\text{Pb}$  shows finite contribution from the asymmetric fission mode at all three excitation energies. The symmetric fission fraction is compared with the recent measurements in the preactinide region. The values of symmetric fission component shows different characteristic clustering for proton induced fission and heavy ion induced fission. These measurements along with recent measurements [7, 8] will help to understand the fission process in pre actinide region and will provide new constrains to theoretical models.

### References

- [1] M. G. Itkis et al., Sov. J. Nucl. Phys **47**, 4 (1988).
- [2] A. N. Andreyev et al., Phys. Rev. Lett. **105**, 252502 (2010).
- [3] M. Warda et al., Phys. Rev. C **86**, 024601 (2012).
- [4] K. Mahata et al., Phys. Lett. B **825**, 136859 (2022), 2007.16184.
- [5] A. Jhingan, Pramana **85**, 483 (2015).
- [6] E. M. Kozulin et al., Phys. Rev. C **105**, 014607 (2022).
- [7] A. A. Bogachev et al., Phys. Rev. C **104**, 024623 (2021).
- [8] B. M. A. Swinton-Bland et al., Phys. Rev. C **102**, 054611 (2020).
- [9] K.-H. Schmidt, B. Jurado, C. Amouroux, and C. Schmitt, Nuclear Data Sheets **131**, 107 (2016).